

Statistical tests for the distribution of surface wind and current speeds across the globe

Salvatore Campisi-Pinto^a, Kaushal Gianchandani^b, Yosef Ashkenazy^{a,*}

^a*Department of Solar Energy and Environmental Physics, BIDR, Ben-Gurion University, Midreshet Ben-Gurion, Israel*

^b*The Fredy and Nadine Herrmann Institute of Earth Sciences, The Hebrew University of Jerusalem, Jerusalem, Israel*

Abstract

The distribution of surface winds and currents is important from climatic and energy production aspects. It is commonly assumed that the distribution of surface winds and currents speed is Weibull, yet, previous studies indicated that this assumption is not always valid. An inaccurate probability distribution function (PDF) of wind (current) statistic can lead to erroneous power estimation; thus, it is necessary to examine the accuracy of the PDFs employed. We propose statistical tests to check the validity of an assumed distribution of wind and current speeds. The main statistical test can be applied to any distribution and is based on surrogate data where the different moments of the data are compared with the moments of the surrogate data. We applied this and other tests to global surface wind and current speeds and found that the generalized gamma distribution fits the data distributions better than the Weibull distribution. The percentage of locations that fall within the confidence level of the assumed distribution varies with the moment. The third moment is used to estimate the potential power of winds and currents—we find that 89% (95%) of the wind (current) grid points fall within the 95% confidence interval of the generalized gamma distribution.

Keywords: surface winds, surface currents, speed statistics, Weibull distribution, generalized gamma distribution

*corresponding author

Email address: ashkena@bgu.ac.il (Yosef Ashkenazy)

1. Introduction

Surface winds and surface ocean currents play a crucial role in regulating the weather and climate systems. Driven by the energy of the Sun, winds are responsible for movement of air across the globe. Winds and currents span a wide range of temporal and spatial scales. By forcing the ocean surface, winds generate surface currents; currents transport ocean water (and hence heat and salt) and, in this way, affect regional and global climatic conditions and circulation. Winds are a major source of ocean kinetic energy—about half of the deep ocean energy (~ 1 TW) is attributed to winds, and the other half, approximately, is attributed to tides [1, 2].

The increasing interest in alternative forms of energy (“green” energy), as a step toward low carbon emissions, has led to a significant increase in the use of wind turbines, to convert the kinetic energy (power) of winds to electric energy (power). However, surface ocean currents have received much less attention as a potential source of energy [3, 4, 5, 6, 7]. Harnessing the kinetic energy of surface ocean currents may be a viable complement to wind energy because surface currents are less erratic and persist for a longer duration of time [8, 9].

Accurate information regarding the distributions of winds and currents can be utilized as a reference for improved ocean and climatic modeling. Accurate estimation of the probability density functions (PDFs) of surface wind and current speeds can be used to reliably estimate their potential power production. Moreover, precise PDFs are required to provide the recurrence time of extreme wind and current events, which are essential from an engineering perspective. Significant progress has been made in finding the PDFs of surface wind and current speeds [10, 11, 12, 13, 14, 15, 16, 17, 18, 19, 20, 21, 22, 23, 24]; however, most of the studies on surface winds and ocean currents accept a simplifying hypothesis that the PDF under consideration follows the Weibull distribution [10, 11, 12, 13, 14, 15, 25, 16, 20, 26, 23] and the Weibull distribution can be used to characterize wind and current speed statistics accurately. A few studies questioned the use of the Weibull distribution as the optimal PDF of surface winds and currents [27, 28, 29, 30, 31] and other distributions have been proposed to characterize the speed data.

For example, the following studies reported different distributions that should be used to fit wind speed data: (i) [32] used a mixture of two Weibull distributions (with two parameters for each distribution and one proportionality parameter) to study the wind statistics over the Eastern Mediterranean.

(ii) [33] studied the wind statistics of 178 off-shore stations (mainly over North America) using the Weibull, Kappa, Wakeby and other distributions, and suggested using different PDFs to describe different aspects of the wind statistics. (iii) [34] studied the wind speed distribution in the area of Palermo using the Weibull, Rayleigh, Lognormal, Gamma, Inverse Gaussian, Pearson type V, and Burr distributions. (iv) [22] studied the ERA-40 wind speed reanalysis data over Europe and found that the generalized gamma (GG) distribution better fits the data. (v) [35] studied wind speed statistics in the inner Mongolia region using the two-parameter Weibull, Logistic, and Lognormal distributions. (vi) [29] used a two-component mixture of Weibull distribution to fit bimodal distributed wind speed. (vii) [36] studied the performance of four different distributions (two- and three-parameter Weibull, Gamma, and Log-normal) to fit wind speed data from Dolný Hričov airport in Slovakia and found that the three-parameter Weibull distribution have the best fit to the data. (viii) [37] used 13 different distributions to study the statistics of hourly wind speed data from 9 stations in the United Arab Emirates and found that the (4-parameter) Kappa and the (3-parameter) Generalized Gamma distributions provide the best fit to the data; mixture of two Weibull distributions (with overall 5 parameters) yielded an even better fit.

The above studies concentrated on specific regions and focused on the statistics of wind speed data. A global analysis of winds above ocean areas was performed, e.g., in [38, 17], which suggested that the Weibull distribution is a good approximation for the PDF of the wind speed. [39, 17] also suggested a stochastic boundary layer model to explain the observed PDF of wind speed. The same author also compared the Weibull statistics (parameters and various moments) using various global and local data sources [18], such as wind estimations that are based on daily SeaWinds scatterometer and the NCEP-NCAR and ECMWF reanalysis.

In contrast to wind speed, the statistics of surface ocean currents have received much less attention. The parameters of the Weibull distribution over the global ocean were estimated based on geostrophic altimetry-based velocities [20, 40]. In addition, [19] discussed the Weibull parameters of the upper equatorial Pacific current speed estimated using six stations' hourly ADCP data. [41] analyzed ocean current statistics from the Gulf Stream (North Carolina shore) and found that the Weibull distribution properly fits the current speed PDF. The parameters of the Weibull distribution of high resolution surface current speeds were also estimated from radar (CODAR)

data of the Gulf of Eilat, Israel [42] and of the Nan-Wan Bay, Taiwan [43]. Other studies [44, 45] investigated surface current velocity components that were based on altimetry data and found that the distribution varies from Gaussian when focusing on small ocean areas to exponential when dealing with extensive ocean areas—they proposed a model to explain their findings. The exponential distribution of the velocity components were also reported in [46], based on oceanic floats and numerical models [46, 47]. We note, however, that the relation between the distribution of the velocity components and the distribution of the current speed, which is the focus of this work, is not trivial, except when considering the idealized identical Gaussian distribution of the velocity components, which will result in the Rayleigh distribution (Weibull distribution with the shape parameter, $k = 2$).

The brief summary above indicates that the statistical analysis of surface winds has received much more attention than that of the surface ocean current speed, and here, we aim to extend the analysis of the latter. In addition, many distributions have been suggested to describe the observed PDF of the wind speed. This situation calls for a standard test. Following the above, the aim of this study is to present a procedure to quantify the level of agreement between an assumed PDF and the actual PDF of both wind and current speed data. The proposed procedure is not specific to either the Weibull or the GG PDF and depends on the moments of interest. We implemented this method on surface winds and currents around the globe using the Weibull and the GG PDFs. We found that the GG distribution more accurately fits the actual distribution of wind and current speed. In addition to the moment-dependent test, we studied other statistical tests.

The paper is organized as follows. Sec. 2 briefly elaborates the data analyzed for this study and in Sec. 3, we present the methodology of the present study. The results are then shown in Sec. 4. Sec. 5 discusses the estimation of the global distribution of the potential power of winds and currents when using the Weibull distribution in comparison to the GG distribution. The study is concluded and discussed in Sec. 6.

2. Data

We analyzed the ERA-Interim (a global atmospheric reanalysis) 6-hourly surface (10 m height) wind speed of the European Centre for Medium-Range Weather Forecasts (ECMWF) [48] from 1979 to 2016. The dataset spans the

entire globe through a geographical grid of size 480×240 (spatial resolution of $3/4^\circ \times 3/4^\circ$).

The surface currents were acquired using satellite altimetry and made available by the Copernicus—Marine Environment Monitoring Service (CMEMS), <http://marine.copernicus.eu> and based on Topex/Poseidon between 1993-01-01 and 2002-04-23, Jason-1 between 2002-04-24 and 2008-10-18, and OSTM/Jason-2 since 2008-10-19; see [49, 50]. The spatial resolution of the altimetry data is much finer than that of the winds (grid size: 1440×720 , spatial resolution of $1/4^\circ \times 1/4^\circ$); still, the temporal resolution is one day. The data spans 24 years, from 1993 to 2016. Both the datasets are freely available online and were download from the respective websites of ECMWF and CMEMS.

3. Methodology

The Weibull PDF is a two-parameter distribution,

$$f(x; \lambda, k) = \frac{k}{\lambda} \left(\frac{x}{\lambda}\right)^{k-1} e^{-(x/\lambda)^k}, \quad (1)$$

where $x \geq 0$, and λ and k are the scale and shape parameters, respectively. The Weibull distribution reduces to the Rayleigh distribution when $k = 2$ and to the exponential distribution for $k = 1$. The GG PDF is a generalization of the Weibull PDF and has three parameters, λ , k , and ε

$$f(x; \lambda, k, \varepsilon) = \frac{1}{\Gamma(\varepsilon)} \frac{k}{\lambda} \left(\frac{x}{\lambda}\right)^{\varepsilon k - 1} e^{-(x/\lambda)^k}, \quad (2)$$

where also here $x > 0$ and $\Gamma(\varepsilon)$ is the gamma function. The GG distribution reduces to the Weibull distribution for $\varepsilon = 1$ and to the gamma distribution for $k = 1$.

Figure 1(a),(b) depicts the Weibull PDFs for $\lambda = 1$ (scale parameter) and for different values of the shape parameter, k . The PDF decays faster for a larger k and, in this way, controls the “shape” of the PDF; the parameter λ only shifts the distribution along the x axis without altering the shape of the distribution. In Figure 1(c),(d), we present the GG PDF for $\lambda = 1$ and for $k = 1, 2$ and $\varepsilon = 1, 2, 3$. Figure 1(c) shows that in some cases ($k = 1$), the ε parameter also controls the shape of the distribution. Since the GG PDF has three parameters, it can potentially improve the fit to the PDF to the data. In Figures 1(e),(f), we present examples of the PDFs of two geographical locations surface wind speeds. In these examples, both

141 the Weibull and the GG PDFs were fitted to the data using the maximum
142 likelihood criteria. As expected, the GG distribution fits the data better than
143 the Weibull distribution. Furthermore, the value of ε estimated for the GG
144 fit was different than 1. If the time-series had been truly Weibull-distributed,
145 the value of ε would have been about 1. In other cases (such as the case of
146 Figure 1(f)), neither the Weibull nor the GG PDF properly fit the PDF of
147 the actual wind speed data. The method we propose below aims to identify
148 the locations at which either the Weibull or the GG distribution is suitable
149 to fit the distribution of the data.

150 We used a methodological protocol based on the method of the moments
151 used in conjunction with the method of the maximum likelihood estimation
152 (MLE) [51, 52] to test the validity of the PDF (here Weibull and GG) hy-
153 pothesis for a sample of measurements. The methods, as presented below,
154 were applied to every single time series of the dataset at hand; i.e., the time
155 series of every grid point were analyzed separately.

156 The method of the moments [52], first introduced by Chebyshev in the
157 19th century, is a method of estimating population parameters. Assum-
158 ing a particular distribution, such as Weibull or GG, for a given sample of
159 measurements, the method estimates the sample distribution parameters by
160 solving a system of equations that relates the sample parameters to be esti-
161 mated with the population moments. This method is used in Appendix B
162 to find the Weibull and GG PDF parameters. In contrast, the MLE esti-
163 mates the parameter values that maximize the likelihood function, given the
164 observations—this method finds the best fit (and hence the optimal PDF
165 parameters) to a given observed distribution. The MLE method is used
166 throughout this paper.

167 The test we propose below is valid for any distribution; as an example,
168 we consider the standard distribution for surface wind and current speed, the
169 Weibull distribution. The analysis unfolds into the following steps:

- 170 (i) we start by assuming that the series at hand (x) is indeed Weibull-
171 distributed (WBL);
- 172 (ii) we estimate the distribution parameters λ and k of x based on the MLE
173 method;
- 174 (iii) by using these estimated parameters, λ and k , we generate a large
175 number ($N = 300$) of surrogate Weibull-distributed series S_i for $i =$

- 176 $1, \dots, N$ where the length of each surrogate series is equal to the length
177 of the original series x ;
- 178 (iv) we estimate the first m_{\max} moments (i.e., $m = 1, \dots, m_{\max}$) of each
179 surrogate series S_i where the m^{th} moment is $\mu_m^{S_i} = \langle S_i^m \rangle$ (where $\langle \cdot \rangle$
180 represents the expected value);
- 181 (v) we calculate the first m_{\max} moments of the original series x , μ_m^x ;
- 182 (vi) in parallel, we estimate the 95% confidence intervals (CIs) of each mo-
183 ment CI_m using the 0.025 and the 0.975 quantiles of the distribution
184 of $\mu_m^{S_i}$;
- 185 (vii) we benchmark μ_m^x against the corresponding CI_m of the surrogate data
186 for all the moments. In other words, for each moment, we test whether
187 μ_m^x falls within the boundary values (quantiles) defined by CI_m .

188 If the value of μ_m^x falls within the CI of the m^{th} surrogate moment, CI_m ,
189 the result of the benchmarking is positive, and the null hypothesis is not
190 rejected; otherwise, the null hypothesis is rejected, and the conclusion is that
191 the PDF of the data is not the assumed one. A positive result indicates that
192 the hypothesized distribution, for example the Weibull, is a good approxi-
193 mation of the PDF of the data, for the specific moment at hand. It is worth
194 emphasizing that the method is “moment-dependent” such that the same
195 sample can score a positive result for a given moment and a negative result
196 for a different one. We analyzed several moments for theoretical purposes,
197 while for most practical applications (for instance, wind speed electric power
198 generation), only moments up to three or four are of interest; the Skewness
199 and Kurtosis are related to the first three and four moments respectively
200 and were analyzed in previous studies [like, 19, 17]. Below, we show the im-
201 plementation of the proposed test when assuming the Weibull and the GG
202 distributions.

203 In addition to the general test proposed above, we propose two other
204 tests that are specific to the Weibull and the GG distributions, and these are
205 discussed in detail in Appendix B and Appendix C; we implement these tests
206 on surface wind and current speed data. Essentially, in the first method, we
207 estimate the parameters of either the Weibull or the GG distribution using
208 the MLE, then generate surrogate series based on these parameters, then
209 use the ratio between the different moments to estimate the parameters of

the assumed distribution of both the original data and the surrogate data, and then check whether the moment-based parameters fall within the CI of the surrogate data moment-based parameters—see Appendix B. In the second method, we use the fact that the GG distribution reduces to the Weibull distribution when $\varepsilon = 1$. We estimate the Weibull parameters using the MLE, then use these parameters to generate surrogate series, and then estimate the GG parameters of these surrogate series. The ε parameter of the GG distribution should be scattered around 1; by comparing the ε parameter of the data to the CI of the ε of the surrogate data, one can conclude whether the data is Weibull-distributed or not (see Appendix C). We also applied the standard χ^2 -test and the Kolmogorov-Smirnov test—see Sec. 6.

4. Results

We first show and discuss the estimated Weibull parameters for the surface wind speed and surface current speed. Figure 3 shows the MLE estimated scale and shape parameters, λ and k , over the entire globe. There is a clear difference in the λ of the wind speed over land and over the ocean where λ is much smaller over land due to the weaker winds there. This is since λ is closely related to the mean speed as the mean wind speed is $\langle s \rangle = \lambda \Gamma(1 + 1/k)$, and since $\Gamma(1 + 1/k) \sim 0.9$ for the relevant range of $k = 1 - 5$, λ is proportional to the mean speed; i.e., $\langle s \rangle \approx 0.9\lambda$. Thus, the scale parameter λ is large in regions of enhanced winds, such as storm tracks and over the Antarctic Ocean. Generally speaking, the shape parameter k of the wind speed Weibull distribution is smaller over land although there are some exceptions like Antarctica. We note that the winds over the tropical ocean are characterized by a large k .

Similarly, with reference to the ocean surface currents, the scale parameter λ also reflects the mean current distribution where, for example, the Gulf Stream, the Kuroshio Current, the Equatorial Current, and the Agulhas Current are clearly visible. Unlike the scale parameter λ , the shape parameter k is almost uniformly distributed over the ocean; no trivial geographical pattern can be extrapolated from the distribution of k . The distributions of the scale and shape parameters, λ and k , for the surface wind and current speed are presented in Fig. A.11 where it is clear that the range of k for the currents is smaller in comparison to the k parameter of the winds. This smaller k for the surface currents may be partially attributed to the fact that the surface of the ocean is forced by the wind stress whose value is, at

246 least, the square of the surface wind speed. The zonal mean of the λ and k
 247 parameters of the winds and currents are presented in Fig. A.12 where the
 248 λ of the winds peak at the mid-latitudes of the southern ocean and the λ
 249 of the currents peak at the equator. The shape parameter k of the surface
 250 currents is almost uniformly distributed over almost all latitudes, in contrast
 251 to the large k for the surface winds for latitudes $\sim 40^\circ\text{S}$ and at the tropical
 252 regions. The results described above are similar to the results discussed in
 253 [17] and in [40].

254 The GG distribution is a generalization of the Weibull distribution, and
 255 below, we show and discuss the MLE-fitted GG distribution parameters, λ ,
 256 k and ε . Figure 4 depicts the estimated parameters of the surface wind speed
 257 data. In general, the λ and k parameters of the Weibull distribution (Fig.
 258 3a,b) are comparable to the corresponding GG λ and k parameters presented
 259 in Fig. 4a,b; however, the GG parameters are typically larger and span a
 260 larger range than the Weibull-estimated parameters. This can be more easily
 261 seen in Fig. A.11a,b where the distribution of both λ and k is broader for
 262 the GG parameters. The zonal mean of the estimated parameters shown
 263 in Fig. A.12a,b indicates that while the pattern of the Weibull parameters
 264 is similar to the pattern of the GG parameters, the GG parameters span a
 265 larger range. For example, the value of λ is larger around 50°S - 60°S , where
 266 the GG one is larger than the Weibull one. A similar situation is observed
 267 for the k parameter (shown in Fig. A.12b) where the GG k is much larger
 268 than the Weibull one for the tropics and around 50°S - 60°S and is smaller
 269 than the Weibull one for the high latitudes. The GG ε parameter of the
 270 surface winds is shown in Fig. 4c, and it seems to be larger over land, in
 271 contrast to the k parameter. The relation between the k and ε parameters of
 272 the GG distribution is plotted in Fig. 4d, and it is clear that the two are not
 273 totally independent. The dependence between the two can be approximated
 274 by a power law relation, i.e., $\varepsilon \propto k^{-4/3}$, indicating a large ε for a small k
 275 and vice versa. We have no explanation for this apparent relation. Despite
 276 the above, one should remember that the approximate power law relation
 277 is not strict and that there is variability around this relation, making the
 278 GG distribution a better approximation for the PDF of the observed surface
 279 winds and surface currents; see below. We note that we could not identify a
 280 similar relation for other parameter combinations.

281 We repeated the estimation of the GG distribution parameters for the
 282 surface ocean current speed (Fig. 5). As for the surface wind speed field,
 283 also here the λ and k parameters of the Weibull are similar to the correspond-

284 ing GG parameters, although the latter span a wider range of parameters,
 285 especially for the k parameters (Fig. A.11d,e). In comparison to the GG
 286 parameters of the surface wind speed, those of the surface currents are re-
 287 stricted to a narrower range of parameters, as we observed for the Weibull
 288 parameters of the winds and currents. The zonal mean of the surface cur-
 289 rent speed GG parameters is very similar to the Weibull ones. Large ε and
 290 small k are observed at the high latitudes, but these values could be due to
 291 the partial data coverage, both in space and time, at these latitudes. The
 292 relation of the ε parameter versus the k parameter is presented in Fig. 5d
 293 where the power law relation between the two ($\varepsilon \propto k^{-4/3}$) seems to hold here
 294 as well; however, the variability around this relation is not small, enabling a
 295 better fit of the GG distribution to the observed distribution of the surface
 296 current speed.

297 In Sec. 3 and in Fig. 2, we described a general method to verify whether
 298 a hypothesized PDF properly fits the PDF of data under investigation (in
 299 our case, wind and current speed). This method depends on the moment and
 300 on the prescribed CI. In Fig. 6, we present a map showing whether the third
 301 moment of the data falls within or outside the 95% CI of the third moment of
 302 the surrogate data. We use the third moment as it is often used to calculate
 303 the potential wind power. Fig. 6a,b depicts the results for the surface wind
 304 speed when assuming that the underlying PDF is Weibull (Fig. 6a) and GG
 305 (Fig. 6b). It is apparent that the null hypothesis of the Weibull distribution
 306 is not rejected over the ocean, while over extensive land areas (e.g., North and
 307 South America and Asia), the null hypothesis is rejected such that one cannot
 308 conclude that the underlying distribution is indeed Weibull. The Weibull null
 309 hypothesis is not rejected for 78% of the global area. When assuming that
 310 the GG PDF is the underlying distribution, the situation improves, and the
 311 null hypothesis is rejected only for 11% of the global area (Fig. 6b). Thus,
 312 as expected, the GG PDF better fits the distribution of the surface wind
 313 speed, especially over land. As for the surface current speed (Fig. 6c,d),
 314 here the situation is better, for both the Weibull and the GG distributions,
 315 where 80% (Weibull) and 95% (GG) of the analyzed area falls within the
 316 CI of the assumed distribution. Based the above, one can conclude that
 317 when focusing on the third moment (using the 95% CI), both the Weibull
 318 and the GG distributions are adequate distributions for both the surface
 319 wind and the current speed; the GG distribution performs better than the
 320 Weibull distribution by more than 10%, and thus is a better choice for the
 321 distribution of the data.

322 The ratio (or percentage) of the analyzed global area that falls within
 323 the 95% CI of the assumed distribution (in our case, either Weibull or GG)
 324 depends on the moment; here, we use the standard 95% CI, but obviously, the
 325 ratio will increase for larger CI and decrease for smaller CI. Fig. 7 shows this
 326 ratio as a function of the moment, for the Weibull and GG distributions of
 327 surface winds and surface currents. In general, there is a decreasing tendency
 328 of the ratio as the moment increases. In addition, there are more grid points
 329 that fall within the GG distribution CI (except $m = 1$ for GG winds) than
 330 within the Weibull ones, and the ratio for the surface current speed is larger
 331 than the surface wind speed. The above situation may vary for moments
 332 larger than $m = 7$. The ratio of the area that is within the CI drops to low
 333 values for large moments.

334 In this section, we considered the surrogate data test described in Sec. 3,
 335 which is applicable to general distribution and which tests each moment sep-
 336 arately. In Appendix B and Appendix C, we present results that are specific
 337 to the Weibull and the GG distributions, where we use a set of moments to
 338 test the null hypothesis of underlying Weibull or GG distributions. These
 339 results indicate that a much smaller analyzed global area can be associated
 340 with the Weibull or the GG distribution. In addition, the χ^2 -test and the
 341 Kolmogorov-Smirnov test yielded a limited area that falls within the CI; see
 342 Sec. 6 and Figs. 9, 10.

343 5. Winds and Oceans — Power Reservoirs

344 Apart from being pivotal to the dynamics of the ocean and the at-
 345 mosphere, winds and currents are of economic importance. In particular,
 346 there is an increasing trend toward the use of green energy [53], to de-
 347 crease greenhouse gas emissions (particularly carbon dioxide) into the at-
 348 mosphere. Worldwide, wind turbines generate several hundred gigawatts of
 349 electrical power with China's contribution being the highest, about 30%; see
 350 <https://www.worldenergy.org/data/resources/>.

351 Winds, however, are not a stable source of electrical power due to their
 352 high spatial and temporal variability [54]. Energy can be harvested from the
 353 ocean through, for example, ocean waves, ocean currents [3, 4, 5, 6], ocean
 354 temperature [55], and tides. Marine energy devices, such as ocean current
 355 turbines, tidal turbines, ocean thermal energy converters, wave energy con-
 356 verters, and in-stream turbines, hold a huge potential for the generation of
 357 green energy.

Accurate knowledge of the distribution of both winds and currents is vital for cost-effective harnessing of the power available through these sources. The power per unit area generated from flowing fluid is [26, 56, 57, 58]:

$$P = \frac{1}{2}\rho\langle U^3 \rangle \quad (3)$$

where ρ is the density of the fluid, and $\langle U^3 \rangle$ is the third moment of the speed of the fluid under consideration.

To compare the performances of the Weibull and GG distributions in estimating the power, the percentage error in the power per unit area was calculated. More precisely, we computed the difference between the estimated power and the observed power (using either the Weibull or the GG estimated distributions) relative to the observed power, $\epsilon = \frac{P_{\text{Weibull or GG}} - P_{\text{observed}}}{P_{\text{observed}}}$. As is evident from Fig. 8, the GG distribution resulted in a more accurate estimate of the power per unit area to the actual value for both winds and currents. Fig. 8c,f, clearly shows that both the Weibull and GG distributions usually underestimate the power per unit area that can be generated by winds and currents. In addition, the distribution of the GG relative error is centered around the zero value, while the Weibull one is much wider, indicating smaller error when using the GG distribution. A comparison between Fig. 6 and Fig. 8a,b,d,e indicates, as expected, that the relative error is (relatively) large (indicated by the green-yellow colors in Fig. 8a,b,d,e) mostly over the regions that fall outside the CI (shown by the green color in Fig. 6), supporting the moment-based test we proposed above. We note, however, that in any case, the relative error is not large and typically is much smaller than 4%.

The use of the Weibull distribution as an approximation for the observed wind and current speed distributions may result in an inaccurate estimation of the power available for extraction for a particular location. The GG distribution instead provides a better estimate regarding the potential wind/current power. Other distributions that were not examined here may provide an even better estimation of the potential power.

6. Summary and conclusions

It is commonly assumed that surface winds and surface sea currents can be accurately modeled by Weibull probability density function over any given geographic location. In this study, we propose a method to test the validity of this assumption; in addition, an alternative distribution (namely the

Generalized Gamma) was tested. Specifically, we analyzed global 10 m surface wind speed ERA-Interim reanalysis data (6 hour interval from 1979 to 2016) and surface, altimetry based daily currents speed dataset (from 1993 to 2016).

At each grid point the tests were implemented as follows: (i) the parameters of the assumed distributions (Weibull and GG) were fitted to the available time series by the MLE method; (ii) the estimated parameters were used to generate a large number of surrogate (synthetic) data; (iii) the moments of the surrogate data were benchmarked against the moment of the original data; if the estimated moment of the original data falls within the confidence interval of the corresponding moment of the surrogate data then, for that moment, the distribution was regarded as truly Weibull (or GG depending on the initial hypothesis) such that the series passed the test (for that moment).

Overall, results showed that the GG distribution was likely to provide a better fit than the Weibull distribution for both winds and currents on a larger portion of geographical locations. In particular, with reference to the third moment of the data (which is used to calculate the potential power of winds and currents) results indicate that the portion of wind speed series passing the tests were respectively 78% when using a Weibull initial hypothesis and 89% when using GG hypothesis; on the other hand, the portion of sea current grid points passing the test were respectively 80% when using the Weibull hypothesis and 95% when using the GG hypothesis. It is worth reminding that the Weibull is a particular case of the GG distribution, when ε is about 1, therefore under appropriate conditions, both Weibull and GG distribution can fit accurately the same data.

In addition to the statistical test discussed above, which is valid for any given PDF, we applied another test that is specific to the Weibull and the GG distributions; see Appendix B and Appendix C. This approach (as described in Appendix B) resulted in a smaller percentage of geographical locations that fell within the CI of the surrogate data. Using this approach, we showed in Appendix C that only a small fraction of the available series ($\sim 10\%$) was truly Weibull. Thus, for a large number of geographical locations, we cannot conclude that the Weibull or the GG were the best assumptions for wind and current speed; conversely, distributions other than Weibull and GG may provide a better fit to the particular data at hand.

We also performed standard statistical tests including the χ^2 -test [59, 60] and the Kolmogorov-Smirnov test [61] as applied on a restricted dataset refer-

ring to Denmark—see, e.g., [13]. These approaches are completely different from the above mentioned tests. In particular, with reference to the χ^2 -test, one basically sums the differences between the observed and the expected frequencies over the observed ranges of measured speeds. Therefore, even a small difference on the density estimated at the tail of the distribution can result in a large overall difference between the empirical and the theoretical distributions. According to the χ^2 -test, results indicate that only a very small fraction of the global area falls within the CI interval of the theoretical PDF, indicating that only in a small portion of surface winds and currents are accurately approximated by Weibull (or GG) distributions (where the GG performs better than the Weibull). Results suggest that the tails of the observed distributions had a large impact on the test statistics; in practice, both the Weibull and the GG distributions were less accurate hypothesis for the highest regimens of wind and current speed.

In the Kolmogorov-Smirnov test, one basically computes the maximal difference between the observed and expected cumulative distributions where a larger difference indicates larger dissimilarity between the two distributions. Large differences are expected close to the center of the PDFs (where the PDFs are maximal), such that the Kolmogorov-Smirnov test is more sensitive to the central part of the distributions. The results of this test are presented in Fig. 10. In this case the percentage of the area falling within the 95% CI interval are much higher than what we obtained for the χ^2 -test. In particular, the GG assumption yielded an area that is twice as large as the area obtained when using the Weibull assumption. In addition, when comparing the test statistics of surface wind speed against surface current speed, the current speed were likely to behave much better, in such a way that the Weibull and the GG assumptions were more accurate for currents than winds.

We translated these tests and assumptions into some of their practical consequences by calculating the potential power generated by surface winds and currents when assuming that the underlying distributions are either Weibull or GG. We estimated the error associated with calculations based on the third moment of the assumed distribution (either Weibull or GG) versus the expected power calculated from the original data. Results indicate that the magnitude of the errors associated with GG distributions are smaller than the errors associated with Weibull assumptions. Moreover, it is worth mentioning that in the context of this study, we focused on the analysis of low moments tested within the standard 95% CI interval. When considering higher moments and different CI intervals, results can change drastically.

467 Tuning the sensitivity of the statistical tests should be tailored to the specific
468 application at hand.

469 In summary, we presented a general procedure to quantify the level of
470 agreement between an assumed PDF and the actual PDF of the wind and
471 current speed data. This procedure is based on comparison between the mo-
472 ments of the original and those of random time series which has the distribu-
473 tion of the assumed distribution. Other statistical tests were also presented
474 and discussed. We found that the GG distribution more accurately fits the
475 actual distribution of wind and current speed around the globe. We obtain
476 better power estimation when using the GG distribution.

477 In this paper we used wind and current reanalysis time series as an ap-
478 proximation of in-situ measures. A potential limitation of this approach
479 is inherent to the very nature of the data that we used for the statistical
480 tests. However it is worth noticing that in-situ measurements are not evenly
481 distributed around the globe, often, highly accurate observations are concen-
482 trated in some countries, while in other regions, in-situ measurements are
483 very sparse, inaccurate or missing all together. In addition, observed mea-
484 sures over different location may not have the same temporal resolution, may
485 not overlap over the the same time period, limiting or completely impairing
486 the feasibility of a global analysis. Taken all this into consideration, reanal-
487 ysis appeared to be an optimal choice for a global analysis. Yet, reanalysis
488 data not always accurately estimate real winds. In addition, the surface cur-
489 rent speeds we analyzed are based on remotely sensed daily altimetry data
490 which are based on the assumption of geostrophy, which is not always accu-
491 rate. Thus, we plan to analyze in-situ measurements of both surface winds
492 and surface currents from different location around the globe and to com-
493 pare these to the results reported here. Moreover, here we focused on *surface*
494 winds and currents and in the future we plan to analyze the statistical prop-
495 erties of winds and currents of other vertical levels, both in the ocean and in
496 the atmosphere; see, e.g., [23]. This can be performed on reanalysis data as
497 well as on measured data. The vertical component of the wind and current
498 vectors is related to the horizontal components via the continuity equation
499 and we are planning to study the relation between these two. It will be also
500 interesting if and how the parameters of the distributions vary with time;
501 this can be accomplished but studying the CMIP5 models in recent history
502 and under future different climate change scenarios.

503 In conclusion, one can ask: are surface wind and current speeds Weibull
504 or GG distributed, if at all? The answer to this question is complex as it

505 depends on the method of analysis and on the moment (or set of moments)
 506 of interest (where different application may focus on different moments).
 507 When focusing on low moments (smaller or equal to 3), we concluded that
 508 the GG distribution was likely to be a more accurate approximation of the
 509 distribution of the original wind and current speed.

510 Acknowledgments

511 We thank Golan Bel and Amos Zemel for helpful discussions.

512 References

- 513 [1] W. Munk, C. Wunsch, Abyssal recipes ii: energetics of tidal and wind
 514 mixing, *Deep Sea Res.* 45 (1998) 1977–2010.
- 515 [2] C. Wunsch, R. Ferrari, Vertical mixing, energy and the general circula-
 516 tion of the oceans, *Ann. Rev. Fluid Mech.* 36 (2004) 281–314.
- 517 [3] P. Lissaman, The coriolis program., *Oceanus* 22 (4) (1979) 23–28.
- 518 [4] H. P. Hanson, S. H. Skemp, G. M. Alsenas, C. E. Coley, Power from
 519 the Florida Current: A new perspective on an old vision, *Bulletin of the*
 520 *American Meteorological Society* 91 (7) (2010) 861–868.
- 521 [5] A. E. Duerr, M. R. Dhanak, An assessment of the hydrokinetic energy
 522 resource of the Florida Current, *IEEE Journal of Oceanic Engineering*
 523 37 (2) (2012) 281–293.
- 524 [6] X. Yang, K. A. Haas, H. M. Fritz, Evaluating the potential for energy
 525 extraction from turbines in the gulf stream system, *Renewable Energy*
 526 72 (2014) 12–21.
- 527 [7] F. Chen, Kuroshio power plant development plan, *Renewable and Sus-*
 528 *tainable Energy Reviews* 14 (9) (2010) 2655–2668.
- 529 [8] H. L. Bryden, L. M. Beal, L. M. Duncan, Structure and transport of the
 530 Agulhas Current and its temporal variability, *Journal of Oceanography*
 531 61 (3) (2005) 479–492.
- 532 [9] J. R. Lutjeharms, *The agulhas current*, Vol. 2, Springer, 2006.

- 533 [10] C. Justus, W. Hargraves, A. Mikhail, D. Graber, Methods for estimat-
534 ing wind speed frequency distributions, *Journal of applied meteorology*
535 17 (3) (1978) 350–353.
- 536 [11] E. S. Takle, J. Brown, Note on the use of weibull statistics to characterize
537 wind-speed data, *Journal of applied meteorology* 17 (4) (1978) 556–559.
- 538 [12] G. Bowden, P. Barker, V. Shestopal, J. Twidell, The weibull distribution
539 function and wind power statistics, *Wind Engineering* (1983) 85–98.
- 540 [13] K. Conradsen, L. Nielsen, L. Prahm, Review of weibull statistics for
541 estimation of wind speed distributions, *Journal of climate and Applied*
542 *Meteorology* 23 (8) (1984) 1173–1183.
- 543 [14] I. Troen, E. L. Petersen, *European wind atlas*, Risø National Laboratory,
544 1989.
- 545 [15] I. Y. Lun, J. C. Lam, A study of weibull parameters using long-term
546 wind observations, *Renewable Energy* 20 (2) (2000) 145–153.
- 547 [16] K. Ulgen, A. Hepbasli, Determination of weibull parameters for wind en-
548 ergy analysis of izmir, turkey, *International Journal of Energy Research*
549 26 (6) (2002) 495–506.
- 550 [17] A. H. Monahan, The probability distribution of sea surface wind speeds.
551 Part I: Theory and SeaWinds observations, *J. Climate* 19 (2006) 497–
552 520.
- 553 [18] A. H. Monahan, The probability distribution of sea surface wind speeds.
554 part ii: Dataset intercomparison and seasonal variability, *Journal of*
555 *Climate* 19 (4) (2006) 521–534.
- 556 [19] P. C. Chu, Probability distribution function of the upper equatorial
557 pacific current speeds, *Geophys. Res. Lett.* 35 (2008) L12606.
- 558 [20] P. C. Chu, Weibull distribution for the global surface current speeds
559 obtained from satellite altimetry, in: *Geoscience and Remote Sensing*
560 *Symposium*, 2008. IGARSS 2008. IEEE International, Vol. 3, IEEE,
561 2008, pp. III–59.

- [21] J. A. Carta, P. Ramirez, S. Velazquez, A review of wind speed probability distributions used in wind energy analysis: Case studies in the Canary Islands, *Renewable and sustainable energy reviews* 13 (5) (2009) 933–955.
- [22] P. Kiss, I. M. Jánosi, Comprehensive empirical analysis of ERA-40 surface wind speed distribution over Europe, *Energy Conversion and Management* 49 (8) (2008) 2142–2151.
- [23] M. Kelly, I. Troen, H. E. Jørgensen, Weibull-k revisited: "tall" profiles and height variation of wind statistics, *Boundary-layer meteorology* 152 (1) (2014) 107–124.
- [24] P. Drobinski, C. Coulais, B. Jourdier, Surface wind-speed statistics modelling: alternatives to the weibull distribution and performance evaluation, *Boundary-Layer Meteorology* 157 (1) (2015) 97–123.
- [25] J. Seguro, T. Lambert, Modern estimation of the parameters of the Weibull wind speed distribution for wind energy analysis, *Journal of Wind Engineering and Industrial Aerodynamics* 85 (1) (2000) 75–84.
- [26] J. F. Manwell, J. G. McGowan, A. L. Rogers, *Wind energy explained: theory, design and application*, John Wiley & Sons, 2010.
- [27] S. E. Tuller, A. C. Brett, The characteristics of wind velocity that favor the fitting of a Weibull distribution in wind speed analysis, *Journal of Climate and Applied Meteorology* 23 (1) (1984) 124–134.
- [28] E. Bauer, Characteristic frequency distributions of remotely sensed in situ and modelled wind speeds, *International Journal of Climatology* 16 (10) (1996) 1087–1102.
- [29] J. Carta, P. Ramirez, Analysis of two-component mixture weibull statistics for estimation of wind speed distributions, *Renewable Energy* 32 (3) (2007) 518–531.
- [30] M. L. Morrissey, J. S. Greene, Tractable analytic expressions for the wind speed probability density functions using expansions of orthogonal polynomials, *Journal of Applied Meteorology and Climatology* 51 (7) (2012) 1310–1320.

- 593 [31] G. Bel, Y. Ashkenazy, The relationship between the statistics of open
594 ocean currents and the temporal correlations of the wind stress, *New*
595 *Journal of Physics* 15 (5) (2013) 053024.
- 596 [32] S. A. Akdağ, H. S. Bagiorgas, G. Mihalakakou, Use of two-component
597 Weibull mixtures in the analysis of wind speed in the Eastern Mediter-
598 ranean, *Applied Energy* 87 (8) (2010) 2566–2573.
- 599 [33] E. C. Morgan, M. Lackner, R. M. Vogel, L. G. Baise, Probability distri-
600 butions for offshore wind speeds, *Energy Conversion and Management*
601 52 (1) (2011) 15–26.
- 602 [34] V. L. Brano, A. Orioli, G. Ciulla, S. Culotta, Quality of wind speed
603 fitting distributions for the urban area of Palermo, Italy, *Renewable*
604 *Energy* 36 (3) (2011) 1026–1039.
- 605 [35] J. Wu, J. Wang, D. Chi, Wind energy potential assessment for the site
606 of Inner Mongolia in China, *Renewable and Sustainable Energy Reviews*
607 21 (2013) 215–228.
- 608 [36] I. Pobočíková, Z. Sedláčková, M. Michalková, Application of four prob-
609 ability distributions for wind speed modeling, *Procedia engineering* 192
610 (2017) 713–718.
- 611 [37] T. B. Ouarda, C. Charron, J.-Y. Shin, P. R. Marpu, A. H. Al-Mandoos,
612 M. H. Al-Tamimi, H. Ghedira, T. Al Hosary, Probability distributions of
613 wind speed in the UAE, *Energy conversion and management* 93 (2015)
614 414–434.
- 615 [38] E. G. Pavia, J. J. O’Brien, Weibull statistics of wind speed over the
616 ocean, *Journal of climate and applied meteorology* 25 (10) (1986) 1324–
617 1332.
- 618 [39] A. H. Monahan, A simple model for the skewness of global sea surface
619 winds, *Journal of the atmospheric sciences* 61 (16) (2004) 2037–2049.
- 620 [40] P. C. Chu, Statistical characteristics of the global surface current speeds
621 obtained from satellite altimetry and scatterometer data, *IEEE J. of*
622 *Selected Topics in Applied Earth Observations and Remote Sensing* 2 (1)
623 (2009) 27–32.

- [41] A. Kabir, I. Lemongo-Tchamba, A. Fernandez, An assessment of available ocean current hydrokinetic energy near the north carolina shore, *Renewable energy* 80 (2015) 301–307.
- [42] Y. Ashkenazy, H. Gildor, On the probability and spatial distribution of ocean surface currents, *J. Phys. Oceanogr.* 41 (2011) 2295–2306.
- [43] Y. Ashkenazy, E. Fredj, H. Gildor, G.-C. Gong, H.-J. Lee, Current temporal asymmetry and the role of tides: Nan-Wan Bay vs. the Gulf of Elat, *Ocean Science* 12 (3) (2016) 733–742.
- [44] S. T. Gille, S. G. L. Smith, Probability density functions of large-scale turbulence in the ocean, *Phys. Rev. Lett.* 81 (23) (1998) 5249–5252.
- [45] S. T. Gille, S. G. L. Smith, Velocity probability density functions from altimetry, *J. Phys. Oceanogr.* 30 (1) (2000) 125–136.
- [46] A. Bracco, J. Lacasce, C. Pasquero, A. Provenzale, The velocity distribution of barotropic turbulence, *Physics of Fluids* 12 (10) (2000) 2478–2488.
- [47] A. Bracco, E. P. Chassignet, Z. D. Garraffo, A. Provenzale, Lagrangian velocity distributions in a high-resolution numerical simulation of the North Atlantic, *J. Atmospheric and Oceanic Technology* 20 (8) (2003) 1212–1220.
- [48] D. P. Dee, S. Uppala, A. Simmons, P. Berrisford, P. Poli, S. Kobayashi, U. Andrae, M. Balmaseda, G. Balsamo, d. P. Bauer, et al., The ERA-Interim reanalysis: Configuration and performance of the data assimilation system, *Quarterly Journal of the royal meteorological society* 137 (656) (2011) 553–597.
- [49] P. Le Traon, F. Nadal, N. Ducet, An improved mapping method of multisatellite altimeter data, *Journal of atmospheric and oceanic technology* 15 (2) (1998) 522–534.
- [50] N. Ducet, P.-Y. Le Traon, G. Reverdin, Global high-resolution mapping of ocean circulation from TOPEX/Poseidon and ERS-1 and-2, *Journal of Geophysical Research: Oceans* 105 (C8) (2000) 19477–19498.

- 654 [51] K. Pearson, Method of moments and method of maximum likelihood,
655 Biometrika 28 (1/2) (1936) 34–59.
- 656 [52] V. K. Rohatgi, A. M. E. Saleh, An introduction to probability and
657 statistics, John Wiley & Sons, 2015.
- 658 [53] O. Edenhofer, M. Kalkuhl, When do increasing carbon taxes accelerate
659 global warming? a note on the green paradox, Energy Policy 39 (4)
660 (2011) 2208–2212.
- 661 [54] I. Karagali, M. Badger, A. N. Hahmann, A. Peña, C. B. Hasager, A. M.
662 Sempreviva, Spatial and temporal variability of winds in the Northern
663 European Seas, Renewable Energy 57 (2013) 200–210.
- 664 [55] M. S. Mitchell, J. D. Spitler, Open-loop direct surface water cooling and
665 surface water heat pump systemsA review, HVAC&R Research 19 (2)
666 (2013) 125–140.
- 667 [56] J. Twidell, T. Weir, Renewable Energy resources, Routledge, 2015.
- 668 [57] A. S. Bahaj, Generating electricity from the oceans, Renewable and
669 Sustainable Energy Reviews 15 (7) (2011) 3399–3416.
- 670 [58] R.-S. Tseng, Y.-C. Chang, P. C. Chu, Use of global satellite altimeter
671 and drifter data for ocean current resource characterization, in: Marine
672 Renewable Energy, Springer, 2017, pp. 159–177.
- 673 [59] K. Pearson, X. on the criterion that a given system of deviations from
674 the probable in the case of a correlated system of variables is such that it
675 can be reasonably supposed to have arisen from random sampling, The
676 London, Edinburgh, and Dublin Philosophical Magazine and Journal of
677 Science 50 (302) (1900) 157–175.
- 678 [60] W. G. Cochran, The χ^2 test of goodness of fit, The Annals of Mathe-
679 matical Statistics (1952) 315–345.
- 680 [61] A. Mood, F. Graybill, D. Boes, Introduction to the theory of statistics.
681 3rd mcgraw-hill (1974).

682 **Appendix A. The parameter distribution of the Weibull and GG** 683 **distributions**

684 Fig. A.11 shows the distribution of the Weibull PDF parameters λ , k ,
685 for the surface winds and current speed as discussed in the main text and
686 shown in Fig. 3. Similarly, Fig. A.11 shows the distribution of the GG PDF
687 parameters, λ , k , and ε . As discussed in the main text, the scale parameter λ
688 reflects the mean speed; this is roughly consistent with the range and center
689 of the distributions shown in Fig. A.11a,d, which are typically 10 m s^{-1} and
690 10 cm s^{-1} for surface wind and surface current speeds, respectively. In all
691 panels (except Fig. A.11d), the GG estimated parameters span a larger range
692 than the Weibull ones. In addition, the k , and ε parameters span a smaller
693 range for the surface currents. We note that very small and very large k
694 and/or ε probably indicate that other distributions, rather than Weibull or
695 GG, may better approximate the data distribution. When the GG parameter
696 $\varepsilon \approx 1$, the GG PDF reduces to the Weibull PDF, and it is evident from Fig.
697 A.11c,f that only a small portion of the distribution of ε is approximately 1,
698 such that for the majority of the global area, the distribution is not Weibull.
699 We elaborate more on this point below (Fig. B.14).

700 The zonal mean of the different parameters of the Weibull and GG dis-
701 tributions of the surface winds and currents are presented in Fig. A.12. We
702 discuss these results in Sec. 4 of the main text. Also here, the λ parameter
703 reflects the mean wind/current speed and is large at latitudes of large speeds
704 (e.g., for currents at the equator and around $54^\circ S$ for southern ocean winds).
705 It is apparent that there is no clear relation between the λ of the winds and
706 the λ of the currents, suggesting that the wind stress forces the ocean in
707 a non-trivial way and that other sources of energy affect the ocean surface
708 geostrophic currents.

709 **Appendix B. Weibull and GG distribution-specific surrogate data** 710 **test**

711 In the main text (Sec. 3), we described a surrogate data test that can be
712 applied to general distributions, for each moment and independently from
713 other moments. Below, we suggest a test that is specific to the Weibull and
714 the GG distributions; similar tests can be developed for other distributions
715 too. We start by describing the method for the Weibull distribution with its
716 parameters λ and k ; a similar procedure, with the proper adjustments, is then

717 repeated for the GG distribution. Assuming that the time series at hand, x ,
 718 is Weibull-distributed, we apply the following steps for every geographic grid
 719 point:

- 720 (i) Estimate the Weibull distribution parameters, λ and k , of the original
 721 time series using the MLE method.
- 722 (ii) Generate many surrogate Weibull-distributed time series, y , using the
 723 λ and k of step (i).
- 724 (iii) Use the method of moments (MOM) to approximate the λ and k of the
 725 original data x and of the surrogate data y . In the case of a Weibull
 726 process, the m^{th} moment is:

$$\langle x^m \rangle = \mu_m = \lambda^m \Gamma \left(1 + \frac{m}{k} \right) \quad (\text{B.1})$$

727 where $\langle \cdot \rangle$ represents the expected value, Γ is the gamma function, and
 728 λ and k are the parameters to be estimated. Based on the data (or
 729 surrogate data), we find the ratio, $r_{i,j}$ as follows

$$r_{i,j} = \frac{\mu_i^{j/i}}{\mu_j} = \frac{\Gamma \left(1 + \frac{i}{k} \right)}{\Gamma \left(1 + \frac{j}{k} \right)} \quad (\text{B.2})$$

730 where i and j are the indexes of two different moments μ_i, μ_j that are
 731 calculated from the data (or surrogate data). By taking the ratio, we
 732 eliminate λ such that only the k parameter has be found by solving the
 733 transcendental equation (B.2); the λ parameter is then found by Eq.
 734 (B.1) using the first moment, for example.

- 735 (iv) Calculate the 95% CI (as the range of values between the 0.025 and
 736 0.975 quantiles) of the k parameter of the surrogate data estimated in
 737 step (iii).
- 738 (v) Verify whether the MOM-based k parameters of the original data (from
 739 step (iii)) fall within the CI of the surrogate data (step (iv)); if positive,
 740 the null hypothesis is not rejected and the original data can be regarded
 741 as Weibull-distributed; otherwise, the Weibull hypothesis is rejected.

742 We now repeat the method described above for the GG distribution. Ba-
 743 sically, the only difference is in step (iii) above, but, for the sake of complete-
 744 ness, we present the entire procedure from the beginning to end. Starting

745 from the assumption that the time series at hand, x , is GG-distributed, we
746 proceed as follows:

- 747 (i) Estimate the GG distribution parameters λ , k , ε of the original data
748 using the MLE method.
- 749 (ii) Generate a large number of GG-distributed surrogate series, y , using
750 the parameters of step (i).
- 751 (iii) Use the method of moments (MOM) to approximate the GG paramete-
752 ters (λ , k , ε) of the original data x and of the surrogate data y . The
753 m^{th} moment of the GG PDF is:

$$\langle x^m \rangle = \mu_m = \frac{\lambda^m}{\Gamma(\varepsilon)} \Gamma\left(\varepsilon + \frac{m}{k}\right) \quad (\text{B.3})$$

754 where $\langle \cdot \rangle$ represents the expected value, Γ is the gamma function, and
755 λ , k , and ε are the GG parameters to be estimated. Based on the data
756 (or surrogate data), we find the ratio, $r_{i,j}$ as follows

$$r_{i,j} = \frac{\mu_i^{j/i}}{\mu_j} = \frac{\Gamma(\varepsilon)^{1-j/i} [\Gamma(\varepsilon + \frac{i}{k})]^{j/i}}{\Gamma(\varepsilon + \frac{j}{k})}. \quad (\text{B.4})$$

Then, we find the k and ε GG parameters by minimizing the following cost function:

$$f(r_{i_1, j_1}, r_{i_2, j_2}) = \left[r_{i_1, j_1} - \frac{\Gamma(\varepsilon)^{1-j_1/i_1} [\Gamma(\varepsilon + \frac{i_1}{k})]^{j_1/i_1}}{\Gamma(\varepsilon + \frac{j_1}{k})} \right]^2 + \left[r_{i_2, j_2} - \frac{\Gamma(\varepsilon)^{1-j_2/i_2} [\Gamma(\varepsilon + \frac{i_2}{k})]^{j_2/i_2}}{\Gamma(\varepsilon + \frac{j_2}{k})} \right]^2 \quad (\text{B.5})$$

757 where (j_1, i_1) and (j_2, i_2) indicate two different sets of moments. The
758 λ parameter is then found using Eq. (B.3), using the first moment, for
759 example.

- 760 (iv) Calculate the 95% CI (using the 0.025 and 0.975 quantiles) of the k and
761 ε of the surrogate data that were estimated using the MOM (detailed
762 in step (iii)).

763 (v) Verify whether the original datas MOM-estimated parameters fall within
 764 the CI of the surrogate data (step (iv)); if positive, the null hypoth-
 765 esis is not rejected, and the data can be regarded as GG-distributed,
 766 while otherwise, the null hypothesis is rejected, and the data cannot be
 767 regarded as being GG-distributed.

768 We use the same datasets analyzed in the main text (Sec. 3), namely the
 769 ERA-Interim surface winds and geostrophic surface currents that are derived
 770 from altimetry measurements. The above tests were applied to every grid
 771 point separately. The results of the above Weibull MOM method are depicted
 772 in Fig. B.13a,b. The analysis is based on the first and second moments.
 773 The results indicate that the surface wind speed over the tropical ocean,
 774 Antarctica and Greenland are not Weibull-distributed as the k parameter of
 775 the assumed Weibull distribution falls outside the CI interval of the surrogate
 776 data. More generally, 60% of the global area of the k parameter of the Weibull
 777 distribution falls within the CI interval of the k parameter of the surrogate
 778 data. As for the surface currents, the k parameter of 78% of the analyzed area
 779 falls within the CI of the surrogate data. The results presented in B.13a,b
 780 are based on the first and second moments—other set of moments yielded
 781 different results, and the percentage of area that falls within the CI of the
 782 surrogate data decreases as the chosen moments increase; see Eq. (B.2).

783 Fig. B.13c,d,e,f depicts the results of the GG parameters. The analysis
 784 is based on moments $m = 1, 2, 3, 4$. Surprisingly, the more general GG dis-
 785 tribution yielded a much larger area that falls outside the CI interval of the
 786 surrogate data; only for $\sim 28\%$ of the analyzed areas did the k and ε GG
 787 parameters fall within the CI of the k and ε of the surrogate data. This is
 788 also valid for the k and ε GG parameters of the surface currents presented in
 789 Fig. B.13d,f where the area within the CI is $\sim 50\%$. These percentages, both
 790 for wind and currents, are much smaller than the percentages we obtained
 791 for the Weibull distribution (60% and 78% for the k parameters of the as-
 792 sumed Weibull distribution, Fig. B.13a,b) despite the fact that the GG is a
 793 more general distribution (compared to the Weibull distribution) that should
 794 result in a larger area that falls within the CI interval of the surrogate data.
 795 Most probably, these smaller percentages for the GG distribution are related
 796 to the fact that we used four moments ($m = 1, 2, 3, 4$) for the GG analysis
 797 and only two ($m = 1, 2$) for the Weibull distribution; generally speaking,
 798 higher moments yield a smaller area that falls within the CI of the surrogate
 799 data. This is consistent with Fig. 7.

800 In Fig. B.13c,d, we present the results of the k parameter of the GG
801 distribution, while in Fig. B.13e,f, we present the results of the ε parameter
802 of the GG distribution. As expected, the results of the two parameters are
803 very similar, as the method solved the two parameters simultaneously. Thus,
804 it is sufficient to concentrate on one of these parameters to make conclusions
805 regarding the assumed probability.

806 **Appendix C. A method of verifying whether a distribution is in-** 807 **deed Weibull**

808 The GG distribution is a generalization of the Weibull distribution, such
809 that when the ε parameter of the GG distribution is equal to 1, $\varepsilon = 1$, the
810 GG distribution reduces to the Weibull distribution; see Eqs. (1), (2). We
811 use this fact to verify whether an assumed Weibull distribution is indeed
812 Weibull. Assuming that the time series at hand, x , is Weibull-distributed,
813 we apply the following steps:

- 814 (i) Estimate the Weibull distribution parameters, λ and k , of the original
815 data using the MLE method.
- 816 (ii) Generate (many) Weibull artificial time series with the same λ and k
817 and the same length as the original time series.
- 818 (iii) Using the MLE, estimate the GG parameters, λ , k , and the ε of the
819 time series from the previous step. The ε parameter should be scattered
820 around 1, $\varepsilon \approx 1$.
- 821 (iv) Calculate the 95% CI interval of the ε parameter from step (iii).
- 822 (v) Estimate the GG distribution parameters of the original data and check
823 whether the ε parameter of the original data is indeed close to 1 and
824 falls within the CI interval of (iv). If positive, the data can be regarded
825 as Weibull-distributed, while if negative, they are not.

826 The results of the method described above are presented in Fig. B.14.
827 With regards to the surface wind speed, it is apparent that only 8% of the
828 global area falls within the CI interval of $\varepsilon \approx 1$, indicating that only 8% of
829 the globe can be considered as Weibull-distributed. The percentage is even
830 lower for the ocean surface currents where only 7% of the analyzed area falls
831 within the CI of $\varepsilon \approx 1$.

832 We note that in the above test, we assumed that the distribution is either
833 Weibull or GG. It is possible that none of these distributions satisfactorily
834 account for the distribution of the original data. This may be the reason for
835 the low percentage we obtained in this test.

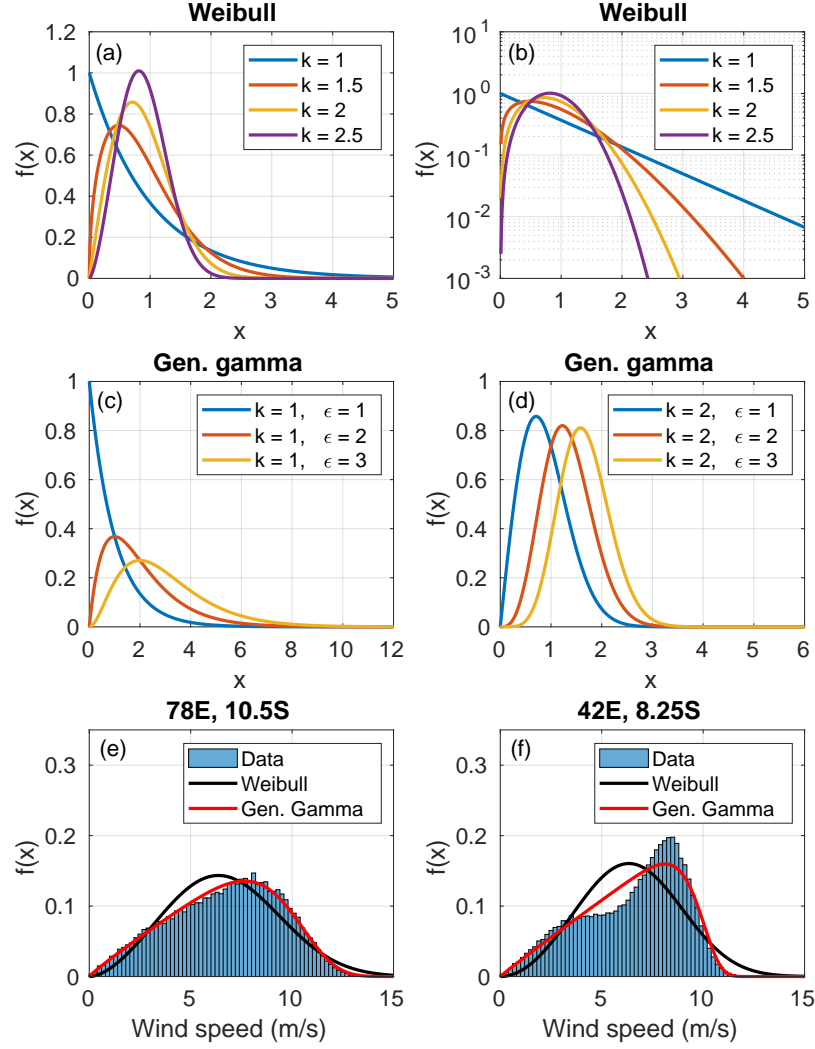


Figure 1: A few illustrative examples of the probability density function (PDF) of the Weibull distribution when the scale and shape parameters are $\lambda = 1$ and $k = 1, 1.5, 2, 2.5$, in (a) regular and (b) semi-log plots. (c) Examples of the PDFs of the GG distribution for $\lambda = 1$, $k = 1$ and $\epsilon = 1, 2, 3$. (d) Same as (c) for $\lambda = 1$, $k = 2$ and $\epsilon = 1, 2, 3$. Two particular instances of sample distributions of surface wind speeds (sampled from 1979 - 2016 at a frequency of 6 hours), as well as the corresponding Weibull and GG approximations at (e) 78°E, 10.5°S [the Weibull parameters are $\lambda = 7.5 \text{ m s}^{-1}$, $k = 2.7$, and the GG parameters are $\lambda = 10.4 \text{ m s}^{-1}$, $k = 6.4$, $\epsilon = 0.3$] and (f) 42°W, 8.25°S [the Weibull parameters are $\lambda = 7.3 \text{ m s}^{-1}$, $k = 3$ and the GG parameters are $\lambda = 10 \text{ m s}^{-1}$, $k = 12.2$, $\epsilon = 0.2$].

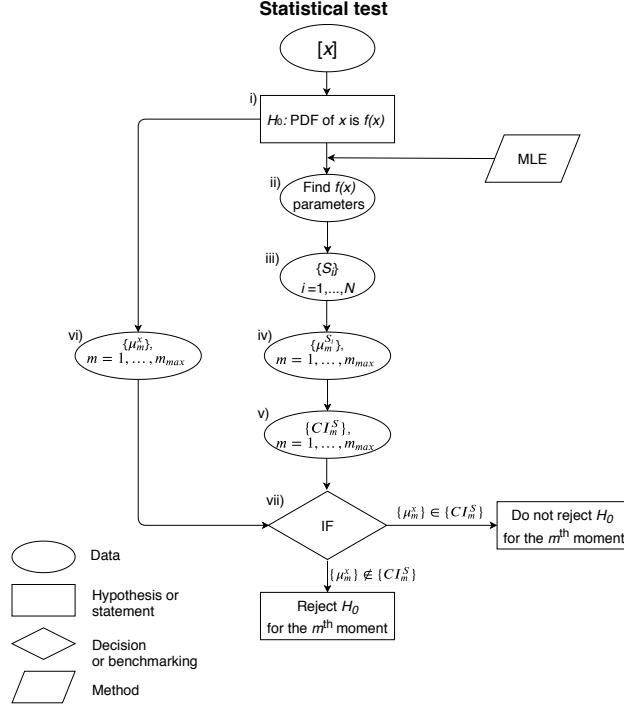


Figure 2: A flow chart showing the various steps of the analysis to test whether a specific assumed distribution $f(x)$ (either Weibull or GG) fits a given time series $[x]$ (in our case surface wind and current speed time series). The chart can be used to (i) test either a Weibull or a GG hypothesis. In step (ii) we apply a method of estimating the parameters of the hypothesis $f(x)$ by maximizing a likelihood function (MLE method). Therefore, using the assumed approximate distribution, (iii) we generate a large number ($i \sim 300$) of surrogate (synthetic) time series $\{S_i\}$ where each series has the same length of the measured data. Thereafter (iv) we calculate $m = 1, \dots, m_{max}$ moments μ_m of each individual surrogate S_i . On the basis of this set of surrogate moments, we estimate in (v) the 0.95 confidence interval (CI) of each moment. In step (vii) we check whether the value of the moment of original data x (calculated in vi) falls within the corresponding confidence interval, CI; the initial null hypothesis H_0 is not rejected if the moment of the original data falls within the CI of the surrogate data while otherwise the null hypothesis is rejected. The method was applied to all series at hand (surface wind and current speed) to test both Weibull and GG distributions but can be generalized to any given distribution that support the MLE method used as the initial estimator of distribution parameters.

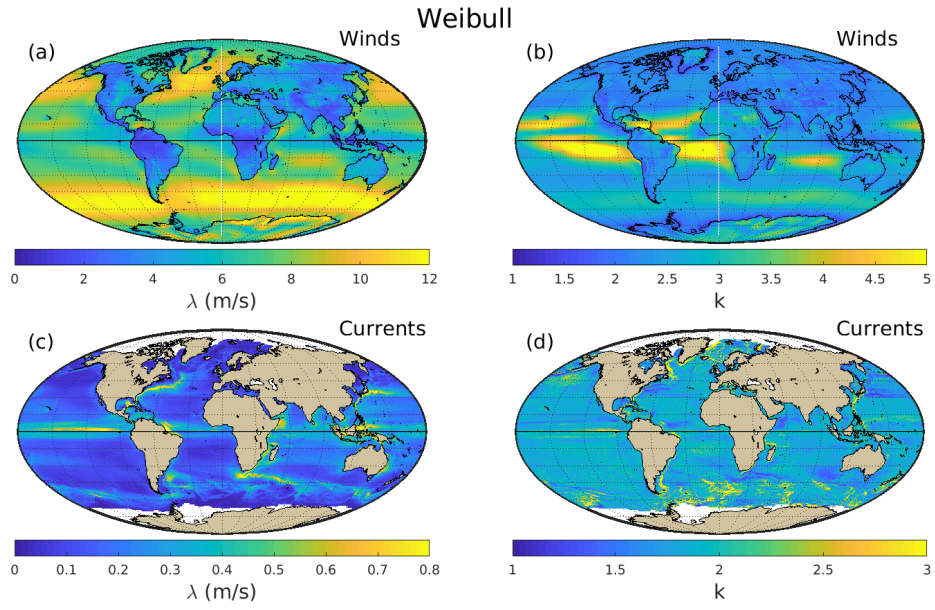


Figure 3: Maps of the Weibull distribution parameters, λ (left panels, in m s^{-1}) and k (right panels) of surface wind speed (upper panels) and surface current speed (lower panels). The parameters were estimated based on the MLE method. The brown color in the lower panels indicates the land regions, while the white color indicates no available data.

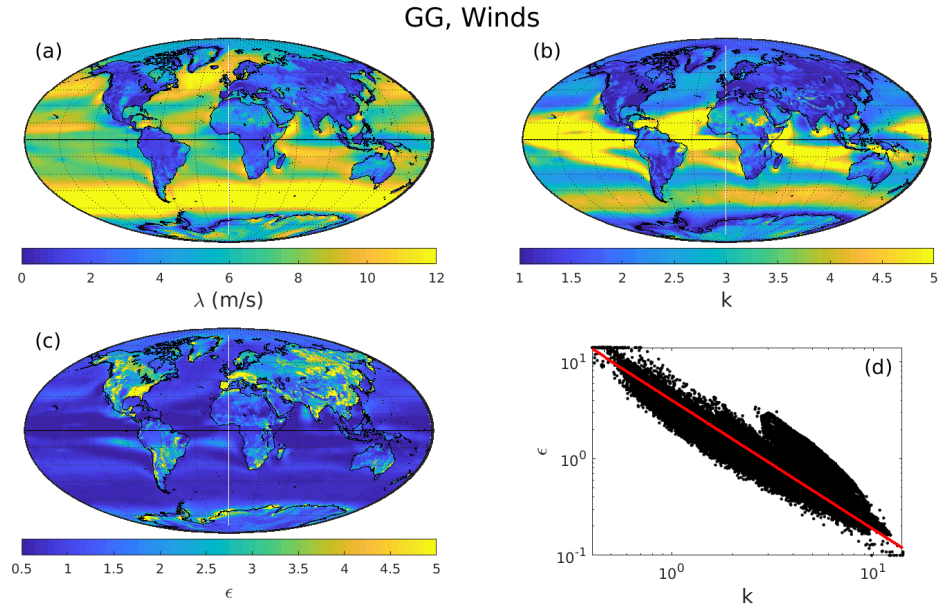


Figure 4: Maps showing the surface wind speed GG parameters (estimated using the MLE) (a) λ (in m s^{-1}), (b) k , and (c) ϵ . (d) The ϵ GG parameter versus the k GG parameter showing that the two are not fully independent—the red line indicates the relation $\epsilon = 4k^{-4/3}$.

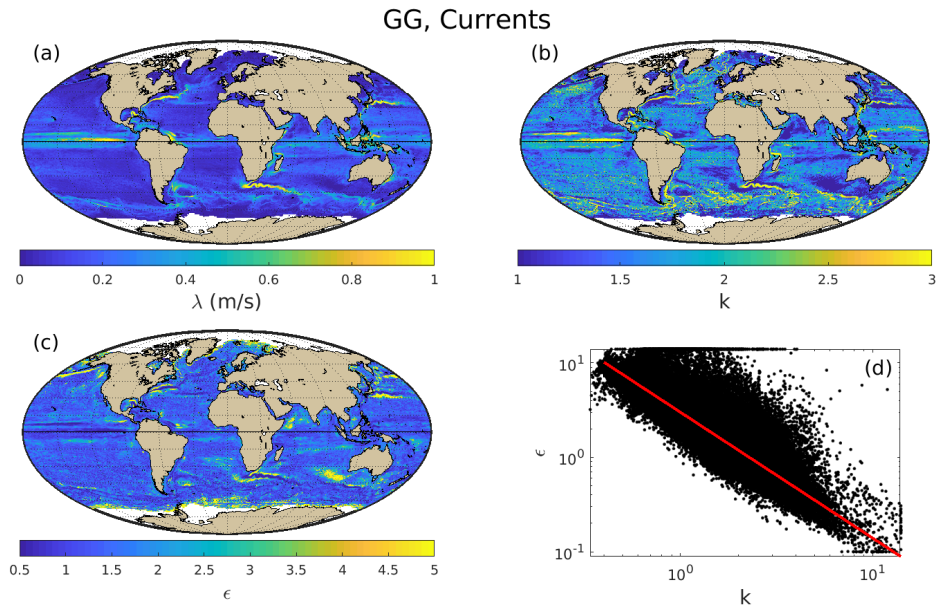


Figure 5: Same as Fig. 4 for the surface ocean current speed. The red line in (d) indicates the relation $\epsilon = 3k^{-4/3}$.

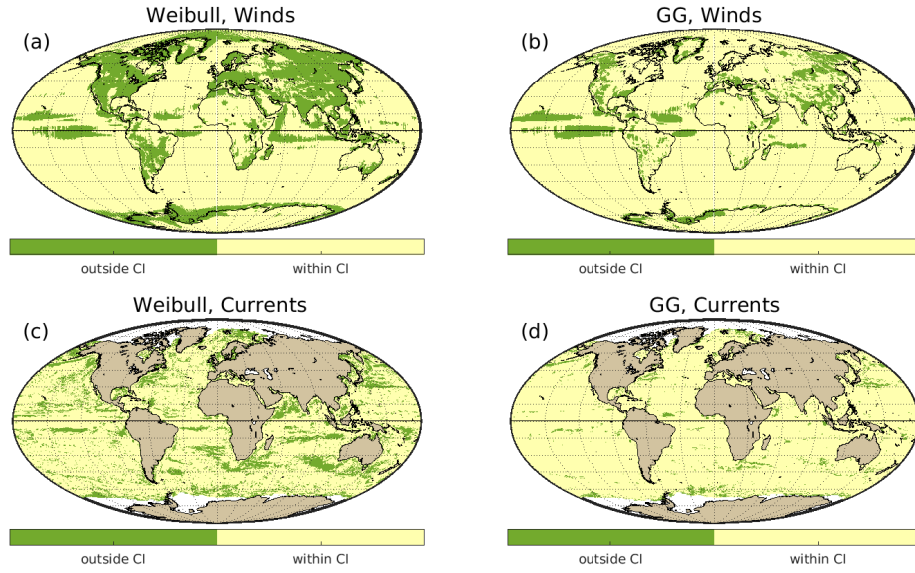


Figure 6: Maps showing the areas where the surface wind speed [(a),(b)] and the surface current speed [(c),(d)] are Weibull-distributed [(a),(c)] or GG-distributed [(b),(d)]: positive (within the 95% CI, yellow), negative (outside the 95% CI, green). The brown color indicates land areas, while the white color indicates no available data. Results are based on the surrogate data method (using the third moment) described in Sec. 3 and in Fig. 2. The percentage of the analyzed area that falls within the 95% CI is (a) 78%, (b) 89%, (c) 80%, and (d) 95%.

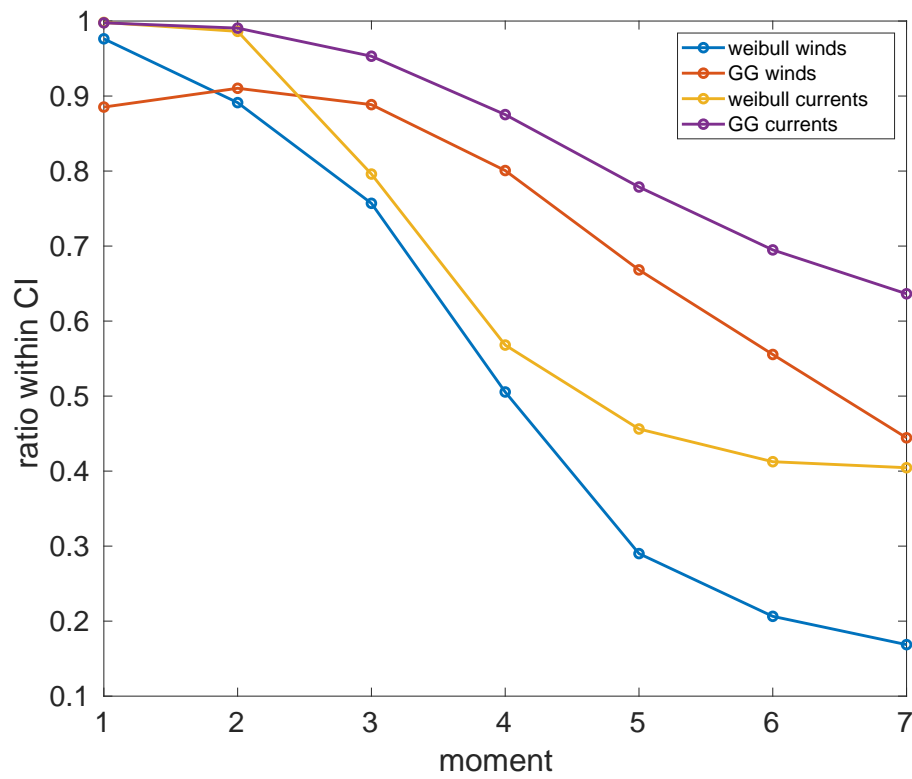


Figure 7: The proportion of the analyzed area that falls within the CI of the assumed distribution for the surface wind and current speed as a function of moment.

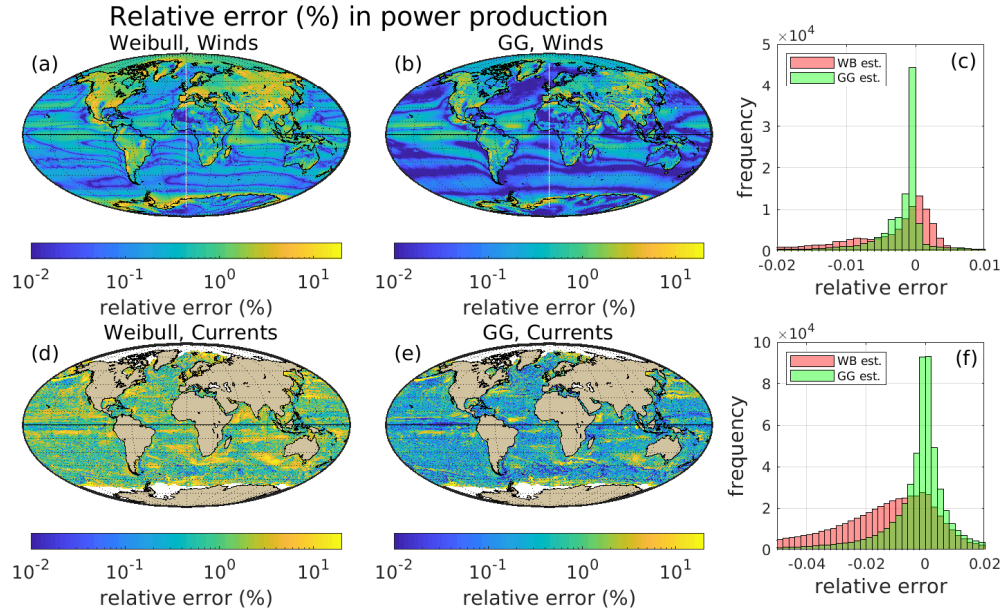


Figure 8: Maps showing the absolute value of the percentage error in the potential wind power per unit area as estimated using the Weibull [(a),(d)] and GG [(b),(d)] distributions for surface winds [(a),(b)] and surface currents [(d),(e)]. Frequency histograms showing the relative errors of the assumed Weibull (WB) and GG distributions for the surface winds (c) and surface currents (f). The red histograms indicate the errors obtained by estimation carried out using the Weibull hypothesis, while the green histograms indicate the error when assuming the GG hypothesis; the overlapping histogram region is indicated by the dark green color.

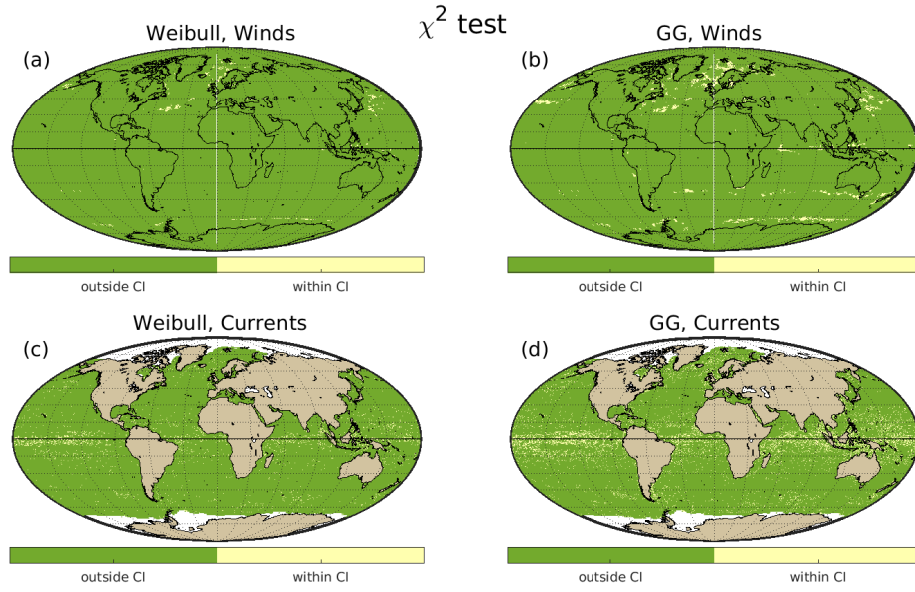


Figure 9: Results of the χ^2 -test. Maps showing the areas where the surface wind speed [(a),(b)] and the surface current speed [(c),(d)] are Weibull-distributed [(a),(c)] or GG-distributed [(b),(d)]: positive (within the 95% CI, yellow), negative (outside the 95% CI, green). The brown areas refer to land areas, while the white color indicates no available data. The percentages of geographic grid points falling within the 95% CI are (a) 0.4%, (b) 1.6%, (c) 2.9%, and (d) 8.3%.

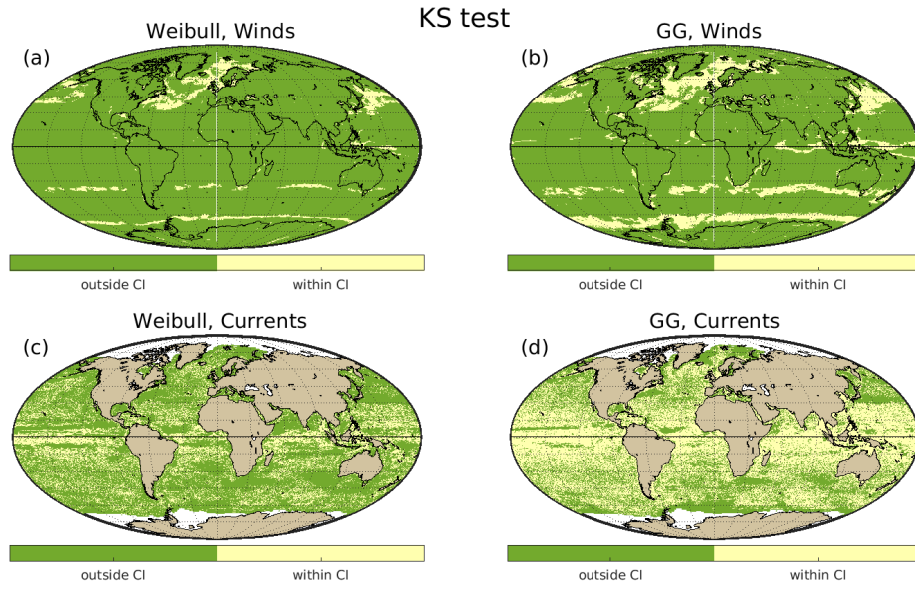


Figure 10: Results of the Kolmogorov-Smirnov test. Maps showing the areas where the surface wind speed [(a),(b)] and the surface current speed [(c),(d)] are Weibull-distributed [(a),(c)] or GG-distributed [(b),(d)]: positive (within the 95% CI, yellow), negative (outside the 95% CI, green). The brown color refers to land areas, while the white color indicates no available data. The percentages of geographic grid points falling within the 95% CI are (a) 4.7%, (b) 11.5%, (c) 29.8%, and (d) 60.1%.

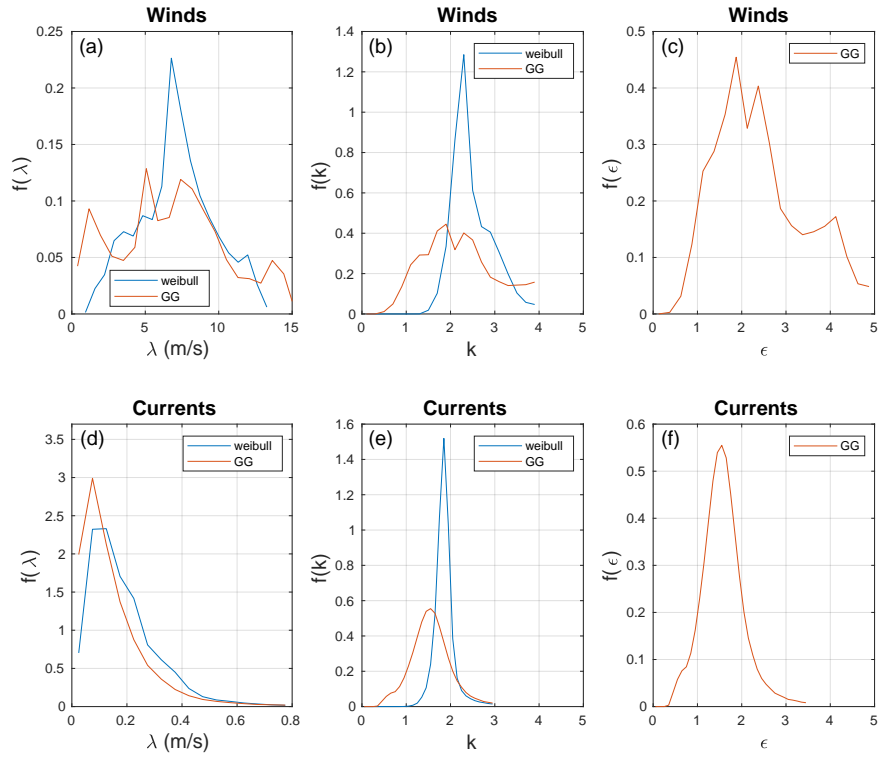


Figure A.11: The distribution of the parameters of the Weibull (blue) and GG (red) distributions estimated using the MLE method, for surface wind speed (upper panels) and surface current speed (lower panels). The λ parameter is shown in panels (a) and (d), the k parameter is shown in panels (b) and (e), and the ϵ parameter is shown in panels (c) and (f).

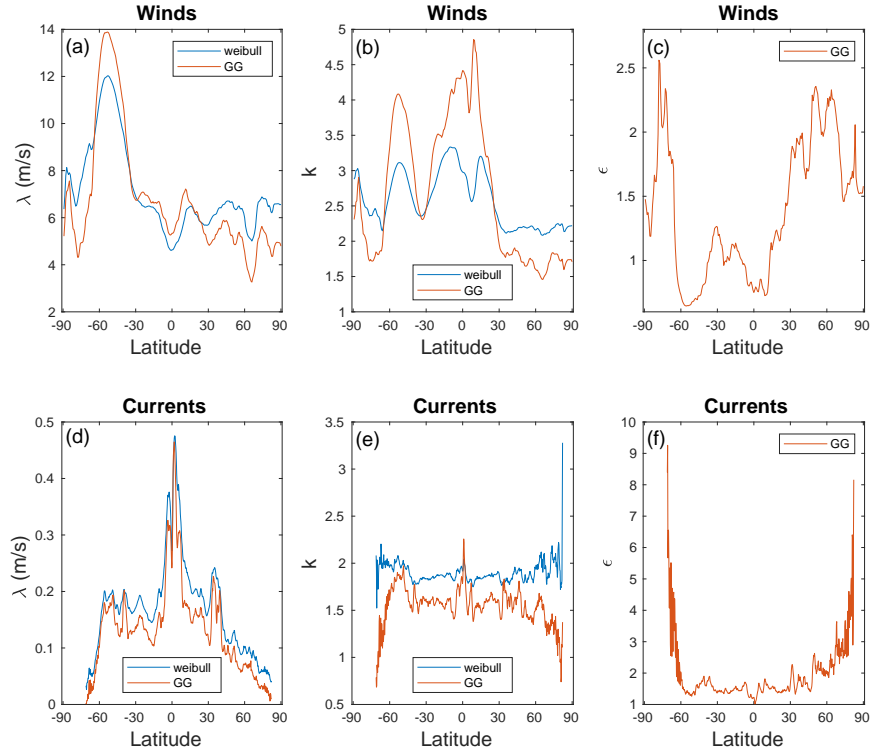


Figure A.12: Zonal mean of the MLE-fitted Weibull distribution parameters (blue) and GG distribution parameters (red) for surface wind speed (upper panels) and surface current speed (lower panels). (a),(d) λ parameter, (b),(e) k parameter, and (c),(f) ϵ parameter.

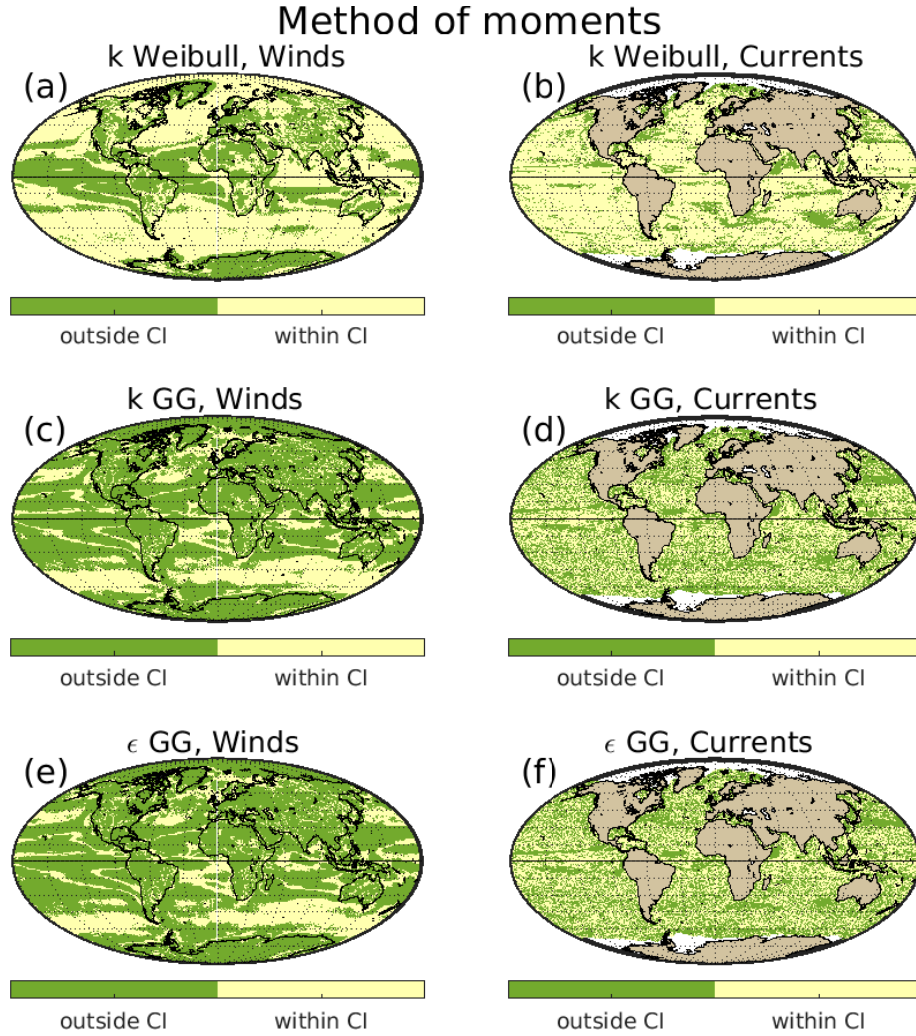


Figure B.13: Maps of the areas where the shape parameter, k , of the data falls within the CI of the k of the surrogate data. The maps are based on the method of moment (Appendix B) assuming a Weibull distribution of (a) surface wind speed and (b) surface ocean currents. (c),(d) same as (a),(b) for the k parameter of the GG distribution and (e),(f) are the same as (c),(d) for the ϵ GG parameter. The brown color in panels b,d,f indicates the land areas, while the white color indicates no available data. The percentage of the analyzed area that falls within the CI is: (a) 60%, (b) 78%, (c) 29%, (d) 50%, (e) 27%, (f) 49%.

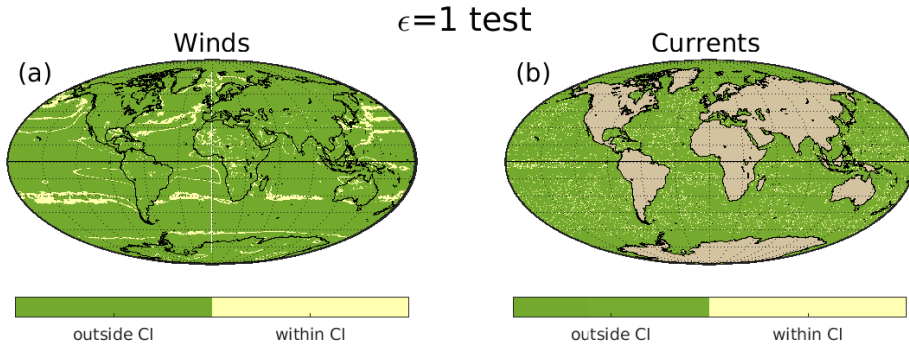


Figure B.14: Maps of the areas where the estimated ϵ of the GG distribution is within (or outside) the CI of the corresponding ϵ of the surrogate data with $\epsilon \approx 1$. Maps for the (a) surface wind speed and (b) surface current speed. Areas with $\epsilon \approx 1$ indicate that the underlying distribution is likely to be Weibull. The brown color in panel b indicates land areas, while the white color indicates no available data. The results are based on whether ϵ lies within the 95% CI of 1 as determined from 300 surrogate time series. The length of the surrogate is the same as the original data. The ratio (in %) of data falling within the CI is (a) 8%, (b) 7%.